Sampling rate and the estimation of ensemble variability for repetitive signals

P. Laguna[1] **L. Sörnmo**[2]

Communication Technology Group, University of Zaragoza, Zaragoza, Spain.
Signal Processing Group, Lund University, Lund, Sweden

Abstract—*The measurement of ensemble variability in time-aligned event signals is studied in relation to sampling rate requirements. The theoretical analysis is based on statistical modelling of time misalignment in which the time resolution is limited by the length of the sampling interval. For different signal-to-noise ratios (SNRs), the sampling rate is derived which limits the misalignment effect to less than 10% of the noise effect. Each signal is assumed to be corrupted by additive noise. Using a normal QRS complex with a high SNR (≃ 30 dB), a sampling rate of approximately 3 kHz is needed for accurate ensemble variability measurements. This result is surprising since it implies that the Nyquist rate is far too low for accurate variability measurements. The theoretical results are supplemented with results obtained from an ECG database of 94 subjects for which the ensemble variability is computed at different sampling rates using signal interpolation. The ensemble variability is substantially reduced (40%) when increasing the rate from 1 to 3 kHz, thus corroborating the results suggested by the theoretical analysis.*

Keywords—*Sampling rate, Ensemble variability, Time-aligned signals, Nyquist rate, ECG database*

Med. Biol. Eng. Comput., 2000, **38**, 540–546

1 Introduction

TIME ALIGNMENT is critical to the analysis of repetitive signals when no synchronisation information is available. Ensemble averaging of time-aligned, repetitive signals is a widely used technique for improving the SNR of various biomedical signals, e.g. for the analysis of cardiac late potentials (BREITHARDT *et al.*, 1991) or evoked potentials of the brain (GEVINS and RÉMOND, 1987). Time alignment turns out to be an even more critical operation when studying ensemble variability of repetitive signals. Although ensemble variability primarily reflects the amount of noise in signals with fixed morphology, it may convey useful information when it is of interest to characterise signals with varying morphology. For example, increased beat-to-beat variability in the QRS complex of the ECG has been suggested as a marker for cardiac electrical instability, possibly related to myocardial ischemia (PRASAD and GUPTA, 1979; BEN-HAIM *et al.*, 1992; NOWAK *et al.*, 1993).

It is well known that misalignment introduces an undesirable low-pass filtering effect in the averaged signal which is caused by noise, signal nonstationarity, and other limitations that affect the performance of the alignment algorithm. This effect must be taken into account when analysing a signal with respect to its high-frequency content. Considering ensemble variability, poor time alignment causes a spurious increase of the variability which is particularly pronounced for waveforms with considerable high-frequency content. Unfortunately, few papers, if any, have studied the latter aspect of time alignment in any detail.

The choice of sampling rate is usually based on knowledge of the signal spectrum, i.e. the Nyquist rate is determined. Recent results indicate, however, that such design considerations may be insufficient when dealing with ensemble variability (LAGUNA *et al.*, 1997; SÖRNMO, 1998). Since sampling limits the alignment precision, the ensemble variability will always include a contribution due to limited time resolution as defined by the length of the sampling interval. It is therefore of interest to study the effect of increased sampling rate, achieved either by sampling the analogue signal at a higher rate or by interpolation of the digitised signal. The present paper develops an analytical approach for studying how the ensemble average (EA) and the ensemble variability (EV) are influenced by various factors: time misalignment, noise, and morphologic variability. The influence of each factor is first treated separately in terms of power measures and then the estimation of morphologic variability in the presence of misalignment and noise is considered briefly. The power measure reflecting ensemble variability is studied in relation to sampling rate. Results based on the theoretical analysis are compared to EV measurements obtained from a high-resolution ECG database.

2 Performance analysis

2.1 *Misalignment in noise-free signals without morphologic variability*

The effect of misalignment is studied under the assumption that $s(t)$ is a repetitive, deterministic signal defined in the time interval $[a, b]$ with a duration of L seconds. The ith realisation in

Correspondence should be addressed to Prof. P. Laguna; email: laguna@posta.unizar.es

First received 2 June 2000

MBEC online number: 20003499

the ensemble of N signals is formed by introducing a random jitter τ_i in the signal, $s(t-\tau_i)$. Neither noise nor morphologic variability are present. The effect of τ_i on the ensemble average is quantified in terms of the error, $e(t)$, between $s(t)$ and the ensemble average $\hat{s}(t)$, i.e.

$$e(t) = s(t) - \hat{s}(t) \tag{1}$$

$$\hat{s}(t) = \frac{1}{N}\sum_{i=1}^{N} s(t-\tau_i). \tag{2}$$

Based on the assumption that the jitter τ_i is small compared to the variations in $s(t)$, the signal $s(t-\tau_i)$ can be approximated by a truncated Taylor series expansion (UIJEN *et al.*, 1979; SHAW and SAVARD, 1995),

$$s(t-\tau_i) \approx s(t) - s'(t)\tau_i + \frac{1}{2!}s''(t)\tau_i^2 \tag{3}$$

Assuming that the random jitter τ_i is zero-mean, i.e. $1/N\sum_{i=1}^{N}\tau_i = 0$ and with variance $\sigma_\tau^2 = 1/N\sum_{i=1}^{N}\tau_i^2$, the first order term of the Taylor approximation is equal to zero and the error $e_\tau(t)$ is therefore described by a second-order term:

$$e_\tau(t) \approx \frac{1}{N}\sum_{i=1}^{N}\left(s'(t)\tau_i - \frac{1}{2!}s''(t)\tau_i^2\right) = -s''(t)\frac{1}{2!}\sigma_\tau^2 \tag{4}$$

Furthermore, the effect of τ_i on the ensemble variability $d_\tau(t)$ is studied in terms of the squared error between $s(t-\tau_i)$ and $\hat{s}(t)$,

$$d_\tau(t) = \sqrt{\frac{1}{N}\sum_{i=1}^{N}(s(t-\tau_i) - \hat{s}(t))^2} \tag{5}$$

Again, by using the first-order approximation it can be shown that the ensemble variability $d_\tau(t)$ is given by:

$$d_\tau(t) \approx \sqrt{\frac{1}{N}\sum_{i=1}^{N}\left(-s'(t)\tau_i + \frac{\sum_{i=1}^{N} s'(t)\tau_i}{N}\right)^2} = s'(t)\sigma_\tau. \tag{6}$$

In order to quantify the effect of misalignment during the interval $[a, b]$, we will study the power of $e_\tau(t)$ and $d_\tau(t)$, respectively,

$$P_\tau^e = \frac{1}{L}\int_a^b e_\tau^2(t)dt \tag{7}$$

$$P_\tau^d = \frac{1}{L}\int_a^b d_\tau^2(t)dt \tag{8}$$

where the index τ implies that the power measure relates to misalignment. By inserting the approximations derived in eqns 4 and 6, the following expressions result,

$$\begin{aligned} P_\tau^e &= \frac{1}{4L}\int_a^b s''^2(t)\sigma_\tau^4 dt \\ &= \frac{\sigma_\tau^4}{4L}\int_{-\infty}^{\infty}(2\pi f')^4|S(f')|^2 df' \\ &= \frac{\sigma_\tau^4}{4MT_s^4}\frac{1}{2\pi}\int_{-\pi}^{\pi}\omega^4|S(\omega)|^2 d\omega \\ &= \frac{\sigma_\tau^4}{4M^2T_s^4}\sum_{k=-M/2}^{M/2-1}\left(\frac{2\pi k}{M}\right)^4|S(k)|^2 \end{aligned} \tag{9}$$

$$\begin{aligned} P_\tau^d &= \frac{1}{L}\int_a^b s'2(t)\sigma_\tau^2 dt \\ &= \frac{\sigma_\tau^2}{L}\int_{-\infty}^{\infty}(2\pi f')^2 S^2(f')df' \\ &= \frac{\sigma_\tau^2}{MT_s^2}\frac{1}{2\pi}\int_{-\pi}^{\pi}\omega^2|S(\omega)|^2 d\omega \\ &= \frac{\sigma_\tau^2}{M^2T_s^2}\sum_{k=-M/2}^{M/2-1}\left(\frac{2\pi k}{M}\right)^2|S(k)|^2 \end{aligned} \tag{10}$$

where $S(f')$ is the Fourier transform of $s(t)$, $S(\omega)$ is its discrete-time Fourier transform, $S(k)$ its discrete Fourier transform, and M is the number of samples in each signal ($L = MT_s$; T_s is the length of the sampling interval). From eqns 9 and 10, it is obvious that misalignment, as described by σ_τ, will affect P_τ^e and P_τ^d differently. If the misalignment factor σ_τ/T_s is less than one (one sample interval), the factor $(\sigma_\tau/T_s)^4$ clearly has a much smaller influence on P_τ^e than the factor $(\sigma_\tau/T_s)^2$ has on P_τ^d. In addition, the energy spectral density $|S(\omega)|^2$ will influence the integrand in different ways, since $|S(\omega)|^2$ is multiplied by ω^4 in P_τ^e and by ω^2 in P_τ^d.

It should be noted that P_τ^e, as well as P_τ^d, depends on the power spectral density distribution of $s(t)$ such that higher frequencies contribute more than lower ones to the error signal $e_\tau(t)$. This observation agrees well with the earlier mentioned low-pass filtering effect associated with misalignment.

2.2 *Noisy signals without misalignment or morphologic variability*

We will now consider the influence of additive, stationary noise $n_i(t)$ on the ensemble average and the ensemble variability under the assumption of perfect time alignment and no morphologic variability. Each realisation in the ensemble is described by $s(t) + n_i(t)$. Again, we consider two power measures for quantifying the influence of noise which here are denoted by P_n^e and P_n^d.

It is well known that the power of the error between $s(t)$ and $\hat{s}(t)$ is equal to the noise variance divided by the number of averaged realisations (ROMPELMAN and ROS, 1986),

$$P_n^e = \frac{\sigma_n^2}{N} \tag{11}$$

where σ_n^2 denotes the noise variance. The corresponding calculation for $d_n(t)$ is, under the assumption that the noise is uncorrelated between realisations, given by:

$$\begin{aligned} d_n(t) &= \sqrt{\frac{1}{N}\sum_{i=1}^{N}\left((s(t)+n_i(t)) - \frac{1}{N}\sum_{j=1}^{N}(s(t)+n_j(t))\right)^2} \\ &= \sigma_n(t) = \sigma_n \end{aligned} \tag{12}$$

and thus the power P_n^d is simply obtained by

$$P_n^d = \sigma_n^2 \tag{13}$$

Obviously, the ensemble variability is much more influenced by noise than is the ensemble average. Assuming that the noise $n_i(t)$ is uncorrelated with the misalignment effect, the total power due to misalignment and noise is given by $P_n^e + P_\tau^e$ and $P_n^d + P_\tau^d$, respectively.

We will now determine the sampling rate for which the misalignment effect is small in relation to the noise effect. To do this, we require that the power due to misalignment is one order of magnitude smaller than that due to noise, i.e.

$P_\tau^e = P_n^e/10$ and $P_\tau^d = P_n^d/10$. The factor 10 was selected to make the misalignment effect sufficiently small in relation to the noise effect. Using these two requirements, we obtain,

$$P_\tau^e = \frac{\sigma_\tau^4}{4L}\int_{-\infty}^{\infty}(2\pi f)^4|S(f)|^2df = \frac{\sigma_n^2}{10\cdot N} = \frac{P_0}{10\cdot N\cdot SNR_l} \tag{14}$$

and, similarly, from eqns 10 and 13 we have that

$$P_\tau^d = \frac{\sigma_\tau^2}{L}\int_{-\infty}^{\infty}(2\pi f)^2|S(f)|^2df = \frac{\sigma_n^2}{10} = \frac{P_0}{10\cdot SNR_l} \tag{15}$$

Here, SNR_l represents the signal-to-noise ratio measured as a linear rather than a logarithmic relation. The power of $s(t)$ is $P_0 = E_0/L$, where E_0 is the signal energy. It is noted that the expressions 14 and 15 represent linear relationships between the SNR and σ_τ.

Assuming that the precision in alignment is entirely determined by the sampling interval, the minimum sampling rate which fulfils eqns 14 and 15 is given by (ROMPELMAN and ROS, 1986)

$$f_s = \frac{1}{2\sqrt{3}\sigma_\tau} \tag{16}$$

2.3 *Signals with morphologic variability but without noise or misalignment*

Morphologic variability is considered to be intrinsic to the signal. To analyse the influence of such variability, we will assume that the signals are noise-free and perfectly aligned in time. Each realisation in the ensemble is described by $s(t) + v_i(t)$, where $v_i(t)$ represents morphologic variability. The corresponding power measures of the error signal, P_v^e, and the ensemble variability, P_v^d, are defined by

$$P_v^e = \frac{1}{L}\int_a^b \frac{d_v^2(t)}{N}dt = \frac{P_v}{N}, \tag{17}$$

$$P_v^d = \frac{1}{L}\int_a^b d_v^2(t)dt = P_v \tag{18}$$

where

$$d_v^2(t) = \frac{1}{N}\sum_{i=1}^{N} v_i^2(t) \tag{25}$$

We will consider a simple model in which morphological variability is assumed to be amplitude variability

$$v_i(t) = a_i s(t) \tag{20}$$

where a_i is modelled by a uniformly distributed random variable within the interval $[-\eta_a, \eta_a]$. Although this model cannot account for sophisticated variability patterns, it is judged to be adequate for modelling variations in the ECG associated with respiration. In this model, it is easily found that $P_v = P_0\eta_a^2/3$ is the power of the variability signal in terms of the amplitude dispersion.

When misalignment and morphologic variability are jointly present, similar reasoning can be made on how to select the sampling rate as in Section 2.2: a sampling rate obtained from the factor 10 requirement (i.e. $P_\tau^e = P_v^e/10$ and $P_\tau^d = P_v^d/10$) is thus viewed as that rate which is required to reliably detect morphologic variability as low as with an SNR $= P_0/P_v$. Eqns 14 and 15 still apply when taking $\text{SNR}_l = P_0/P_v$.

2.4 *Measuring morphologic variability in the presence of noise and misalignment*

It is obvious that measurements of overall ensemble variability, $d(t)$, do not only reflect morphologic variability but time misalignment and noise as well. Therefore, when relying on $d(t)$, it is important to use a sampling rate which ensures that the misalignment effect is sufficiently small. The other step to be taken is to compensate for the ensemble variability $d(t)$ with respect to the noise contribution. This can sometimes be accomplished by estimating the noise variance at a certain time t_0 when the effects due to morphologic variability and misalignment are negligible. The variance estimate is then obtained by $\hat{\sigma}_n^2 \simeq d^2(t_0)$, and a new signal can be defined, $\hat{d}_v^2(t) = d^2(t) - d^2(t_0)$, from which variability measurements with better accuracy can be obtained.

Such a noise compensation procedure has been considered when measuring morphologic variability in the QRS complex (SHAW and SAVARD, 1995). In that case, the isoelectric segment between the end of the P wave and the onset of the QRS complex was considered to contain a t_0 with negligible morphologic variability and without any effect due to misalignment. In other applications as Holter ECG, exercise or pediatrics ECGs where the PQ segment is not stable at all, a better estimate can be obtained from the TP segment. In any case, this estimate should be taken from high-pass filtered signals to avoid biased noise power given by baseline drift or U waves.

3 Results

The choice of sampling rate is first studied from a theoretical point of view relying on the results in Sections 2.1 and 2.2. The signal $s(t)$ is taken as a QRS complex (Fig. 1) acquired with a sampling rate of 1 kHz from a normal subject. The QRS was up-sampled to 100 kHz, using sinc-based interpolation, to avoid effects due to time quantisation. The ensemble contained 100 beats formed by adding to the same QRS different effects (noise, misalignment or variability) and the signal power of each beat was normalised to one ($N = 100$ and $P_0 = 1$, respectively). The theoretical results are supported by measurements on ensemble variability obtained from simulated signals (Section 3.2) as well as from ECG signals (Section 3.3).

3.1 *Theoretical results*

The power measures describing the contributions due to misalignment, noise and morphologic variability for different values of σ_τ, SNR and η_a are presented in Table 1 for the particular QRS in Fig. 1. In this table, the values reveal that the effect of misalignment is between one and three orders of

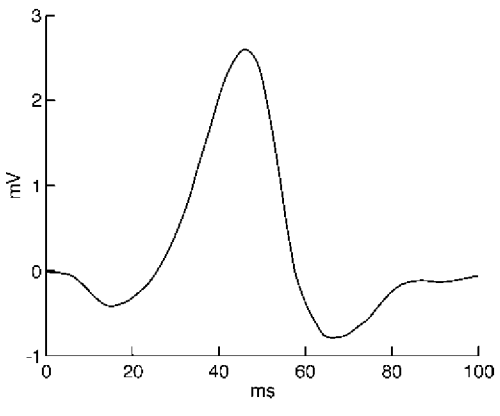

Fig. 1 *The QRS complex used for the study*

Table 1 Power measures for contributions due to misalignment, noise, or morphologic variability independently for the QRS complex in Fig. 1 (N = 100 beats)

σ_τ (ms)	P_τ^e in EA	P_τ^d in EV
4	$4.04 \cdot 10^{-2}$	$2.01 \cdot 10^{-1}$
1	$1.58 \cdot 10^{-4}$	$1.26 \cdot 10^{-2}$
0.288	$1.08 \cdot 10^{-6}$	$0.98 \cdot 10^{-3}$
0.25	$0.62 \cdot 10^{-6}$	$0.79 \cdot 10^{-3}$

(a) Power measures due to misalignment

SNR (dB)	P_n^e in EA	P_n^d in EV
10	10^{-3}	10^{-1}
20	10^{-4}	10^{-2}
30	10^{-5}	10^{-3}

(b) Power measures due to noise

η_a	P_v^e in EA	P_v^d in EV
0.05	$0.83 \cdot 10^{-5}$	$0.83 \cdot 10^{-3}$
0.1	$3.33 \cdot 10^{-5}$	$3.33 \cdot 10^{-3}$
0.15	$7.50 \cdot 10^{-5}$	$7.50 \cdot 10^{-3}$

(c) Power measures due to morphological variability

magnitude smaller in the EA estimation than in the EV estimation. So even if the alignment error σ_τ decreases both indexes, the effect is much more noticeable in the EV signal. It should be noted that the P_τ^e and P_τ^d indexes have contributions also from noise and signal variability. This result suggests a much larger effect of alignment improvement in variability analysis than in signal averaging.

The sampling rate needed to ensure that the misalignment effect is less than 10% of the noise effect is presented in Table 2. This sampling rate is obtained by combining eqn 16 with the power measures in eqn 14 and eqn 15. It is noted from Table 2 that the demands on sampling rate increase when the SNR increases. Moreover, ensemble averaging requires a lower sampling rate than does ensemble variability when the SNR is about 30 dB (typical for high resolution ECG analysis). For example, a sampling rate of $f_s = 1023$ Hz is required for ensemble averaging at an SNR = 30 dB, while a threefold increase is needed for accurate measurements of ensemble variability ($f_s = 3239$ Hz). It should be emphasised that noise also influences the precision of time alignment and, accordingly, the results in Table 2 can be viewed as lower bounds. The variance σ_τ is, in practice, larger due to noise than is indicated by eqn 16.

Table 2 Sampling rate (Hz) which ensures that time misalignment is < 10% of the variability effect

SNR (dB)	EA	EV
0	181	102
10	323	324
20	576	1024
30	1023	3239

3.2 *Simulation results*

Focusing on the ensemble variability power measures, we will now corroborate the results above by simulating the following four ensembles, each with $N = 100$.

1 In the first ensemble, each realisation is formed by the same QRS of Fig. 1 delayed by a zero-mean, Gaussian random variable τ_i. The dispersion is $\sigma_\tau = 0.288$ ms so as to model the dispersion associated with $f_s = 1000$ Hz. (The time delay is quantised to a resolution of 0.01 ms because of the 100 kHz sampling rate.) The resulting ensemble is plotted in Fig. 2*a*.
2 The second ensemble is obtained by adding white, stationary Gaussian noise $n_i(t)$ to $s(t)$ with SNR = 30 dB (Fig. 2*b*).
3 The third ensemble is obtained by assuming that the morphologic variability of $s(t)$ is characterised by eqn 20, a uniformly distributed a_i and $\eta_a = 0.1$ (Fig. 2*c*).
4 Finally, an ensemble is generated which includes all of the above mentioned effects, i.e. $s(t - \tau_i) + n_i(t) + a_i s(t)$ (Fig. 2*d*).

Fig. 3 shows the squared ensemble variability and the corresponding power estimate computed from each of the four above ensembles. It is obvious that the power estimate associated with each of the first three ensembles ($\hat{P}_\tau^d = 0.0011$, $\hat{P}_n^d = 0.0010$ and $\hat{P}_v^d = 0.0034$) agrees well with the corresponding values in Table 1, i.e. $P_\tau^d = 0.0010$, $P_n^d = 0.0010$ and $P_v^d = 0.0033$.

In practice, we are forced to estimate morphologic variability from an ensemble which also contains the undesirable effects due to misalignment and noise (i.e. as described by the fourth ensemble). Straightforward computation of the overall ensemble variability from $d(t)$ gives $\hat{P}^d = 0.0057$ which, after subtraction with the noise power ($\hat{P}_n^d = 0.0010$), produces an estimate of morphologic variability, $\hat{P}_v^{d'} = 0.0047$. Obviously, this estimate is inaccurate since the true morphologic variability is equal to $P_v^d = 0.0033$. This discrepancy is explained by the fact that P_τ^d cannot be neglected with respect to the morphologic variability. Therefore, we will investigate an ensemble with the same variability properties but with a lower dispersion σ_τ, thus corresponding to a higher sampling rate.

From Table 2 we have that a sampling rate of 3239 Hz is needed for proper detection of morphologic variability at an SNR of 30 dB. Using the time dispersion $\sigma_\tau = 0.089$ ms, which corresponds to this sampling rate, the squared ensemble variability and related power estimate are presented in Fig. 4 for each of the four ensembles. It is obvious that the variability due to

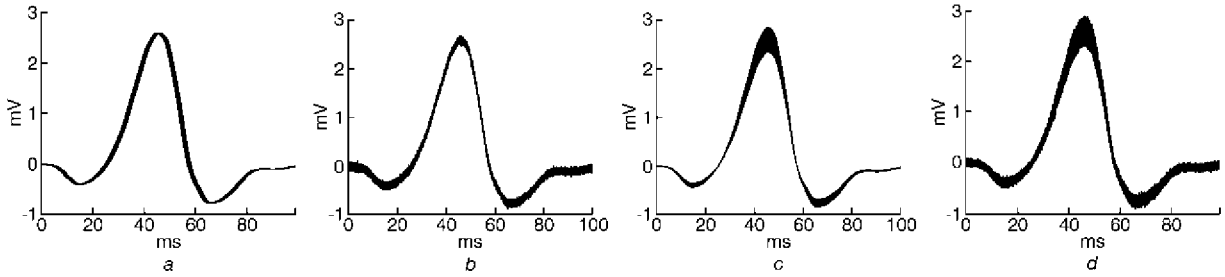

Fig. 2 *QRS signal ensembles with (a) Gaussian delay τ_i with $\sigma_\tau = 0.288$ ms (corresponding to $f_s = 1000$ Hz), (b) additive Gaussian noise at SNR = 30 dB, (c) morphologic variability with uniformly distributed amplitude ($\eta_a = 0.1$), and (d) all three effects combined. In all cases $N = 100$ beats*

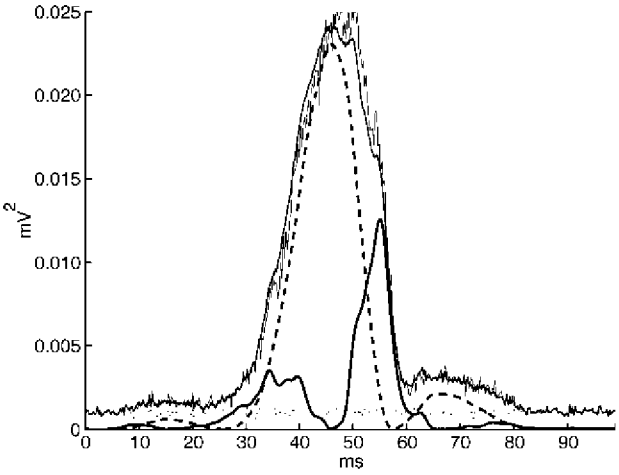

Fig. 3 *Squared ensemble variability for the four ensembles shown in Fig. 2 and the sum of the independently estimated EV ($\hat{d}_n^2(t) + \hat{d}_\tau^2(t) + \hat{d}_v^2(t)$). Note the overall agreement between the total $d^2(t)$ and the sum of the independently estimated EV. The estimated power of each contribution is: $\hat{P}_n^d = 0.0010$, $\hat{P}_\tau^d = 0.0011$, $\hat{P}_v^d = 0.0034$ and $\hat{P}^d = 0.0057$. For more details see text; . . . . $d_n^2(t)$, —— $d_\tau^2(t)$, ---- $d_v^2(t)$, —— $d^2(t)$, —— $d_n^2(t) + d_\tau^2(t) + d_v^2(t)$, SNR = 30 dB, f_s = 1000 Hz*

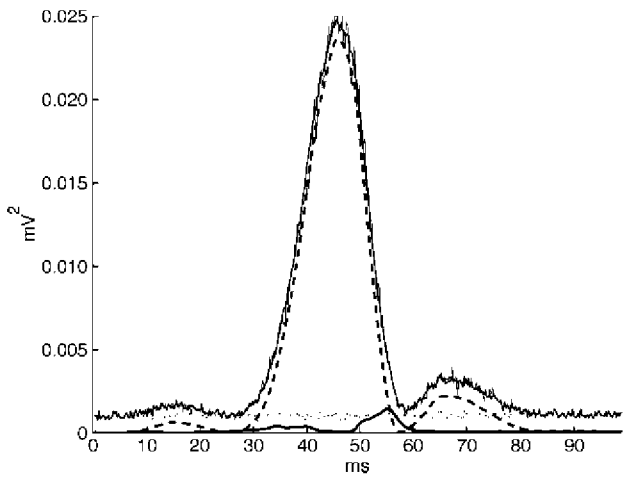

Fig. 4 *Same as in Fig. 3 but with a misalignment of $\sigma_\tau = 0.0891$ ms which corresponds to $f_s = 3239$ Hz. The estimated power of each contribution is: $\hat{P}_n^d = 0.0010$, $\hat{P}_\tau^d = 0.0001$, $\hat{P}_v^d = 0.0035$ and $\hat{P}^d = 0.0046$; . . . . $d_n^2(t)$, —— $d_\tau^2(t)$, ---- $d_v^2(t)$, —— $d^2(t)$, —— $d_n^2(t) + d_\tau^2(t) + d_v^2(t)$, SNR = 30 dB, f_s = 3239 Hz*

misalignment, $d_\tau(t)$, is now much lower than that for 1 kHz in Fig. 3. Repeating the above procedure of subtracting the noise power, an accurate estimate of the morphologic variability results, $\hat{P}_v^{d'} = \hat{P}^d - \hat{P}_n^d = 0.0046 - 0.0010 = 0.0036$, which is very close to the true value 0.0035.

It is noted from Figs 3 and 4 that the agreement between the overall variability $d^2(t)$ and the sum of individual components, $d_n^2(t) + d_\tau^2(t) + d_v^2(t)$, is good. Therefore, the assumption of a lack of correlation between the three components made in Section 3.1 seems reasonable to apply for moderate to high SNRs.

3.3 *Experimental results*

3.3.1 *Database*

Ninety-four non-selected subjects referred for myocardial scintigraphy were included in this study. Thirty-four subjects had no signs of ischemia or infarction. The remaining 60 subjects had signs of ischemia or myocardial infarction or both on the scintigraphy.

The ECG was acquired during rest for five minutes using a standard 12-lead configuration (V_1 to V_6, I, II, III; the augmented limb leads aVR, aVL and aVF were not analysed). The signal was digitised* at a sampling rate of 1000 Hz with an amplitude resolution of 0.6 μV. The amplifier had a bandwidth of 0 to 250 Hz. From each recording, 100 normal sinus beats were selected for time alignment and subsequent ensemble variability measurements. An increase in sampling rate (up-sampling) was achieved by sinc-based interpolation.

3.3.2 *Time alignment method*

Time alignment was based on an *a posteriori*, matched filtering technique which makes repeated use of all beats in the alignment process; the so-called Woody method (WOODY, 1967). In the initial step, all beats are aligned using a matched filter with known impulse response (e.g. taken as the first beat in the ensemble). Having aligned all beats, the ensemble average is taken as the new impulse response and another iteration of the alignment process is performed. The 'alignment/filter update' procedure is repeated until no further time shifts occur between successive iterations. For multilead ECGs, the method processes each individual lead with its corresponding matched filter (SÖRNMO *et al.*, 1998). The filter outputs are then summed together and the time for the maximum amplitude is located from the output and used in the next iteration.

3.3.3 *Reduction in ensemble variability as a function of sampling rate*

The power of the ensemble variability was computed for each lead of the time aligned beat ensemble at sampling rates ranging from 1 to 5 kHz in increments of 1 kHz. The power values were normalised to the 1 kHz value and then averaged over all leads. Finally, the lead-averaged power values were averaged over all 94 subjects. The resulting average reduction in ensemble variability is presented in Fig. 5*a*. It was found that the largest reduction was obtained by increasing the sampling rate from 1 to 2 kHz. Using a sampling rate higher than 3 kHz did not produce much further reduction. This result is in general agreement with the theoretical sampling rate (3239 Hz) which was required to ensure that the misalignment effect was less than 10% of the morphologic variability for the particular QRS complex in Fig. 1. It is also apparent from the standard deviation bars in Fig. 5*a* that a considerable case-to-case variation exists in the degree of reduction. Although the reduction in variability differs considerably from case to case, it reaches a lower limit in all cases around 3 kHz. This observation is concluded from Fig. 5*b* which presents the average behaviour of the difference between successive values for the cases in Fig. 5*a*.

Fig. 6 presents a case in which a considerable reduction occurs in ensemble variability when the sampling rate increases from 1 to 3 kHz. The largest reductions were found in leads V_3 and V_4. It is interesting to observe that the QRS waveforms of these leads also had the steepest slopes (higher high-frequency contribution).

4 Discussion

Historically, the problem of selecting a sufficient sampling rate for ECG analysis has received considerable attention (BERSON, 1976; BARR and SPACH, 1977; ZYWIETZ *et al.*, 1983; BLANCHARD and BARR, 1985). The sampling rate that is

*Equipment by Siemens-Elema AB, Solna, Sweden

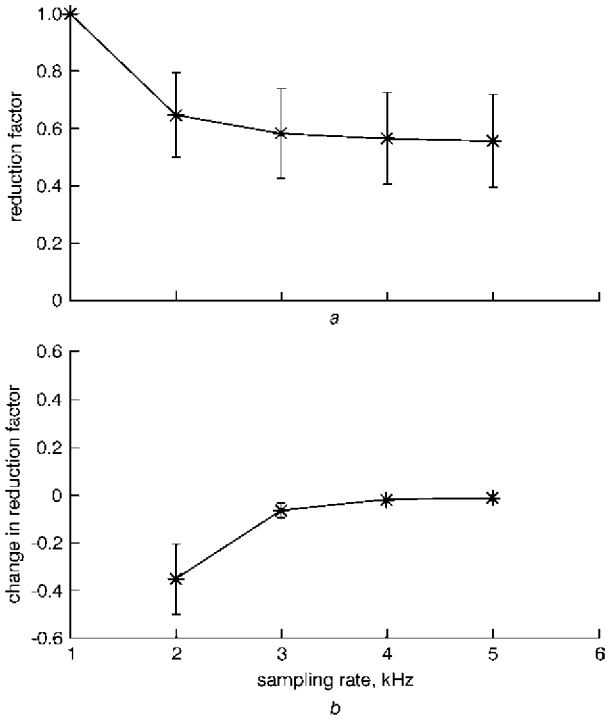

Fig. 5 *(a) Average reduction in the ensemble variability power as a function of sampling rate (the sampling rate is increased in steps of 1 kHz). Values are normalised with the 1 kHz value, averaged over leads for every subject, and finally averaged over the 94 subjects. Bars represent standard deviation across subjects. (b) Average behaviour of the difference between successive values for the cases in (a)*

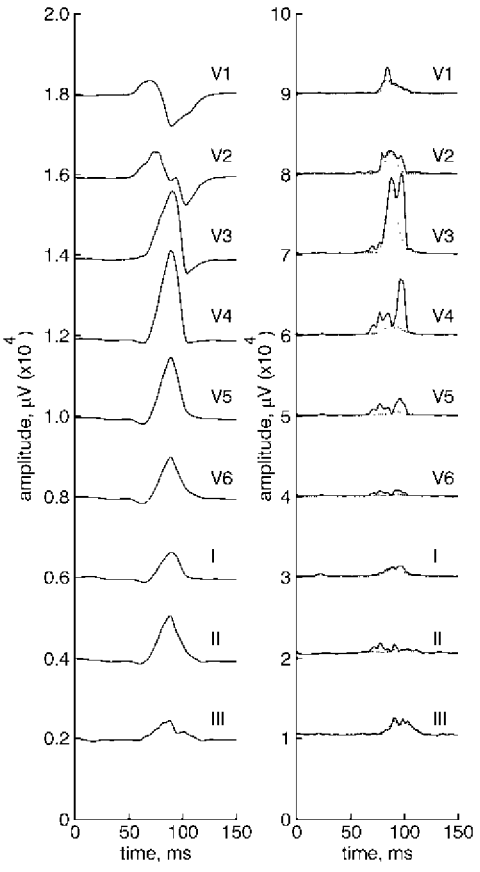

Fig. 6 *Example of ensemble variability reduction when increasing the sampling rate from 1 to 3 kHz. (a) the original ECG leads and (b) the corresponding ensemble variability for a sampling rate of 1 kHz (solid line) and 3 kHz (dotted line)*

suggested depends, to a large degree, on the intended type of analysis. For high-resolution analysis, a rate of 1 kHz is considered sufficient for accurate representation of high-frequency notches and slurs occurring in the QRS complex (BARR and SPACH, 1977). Currently, this rate is commonly used in commercial systems for late potential analysis in which ensemble averaging is performed. A lower sampling rate, e.g. 250 or 500 Hz, can be acceptable for diagnostic purposes where the measurement of different QRS amplitudes and durations are required (BERSON, 1976).

The analysis of paediatric ECGs calls for a sampling rate which may be as high as 4 kHz (YAMAMOTO *et al.*, 1987). In that study, however, different sampling rates were not investigated in a systematic way; only the rates 250 Hz and 4 kHz were investigated. The QRS duration may be as short as 30 ms in newborns and is thus more than three times shorter than in a normal adult. Assuming that the QRS shape of a newborn and an adult are identical, The QRS complex of a newborn, $s_{nb}(t)$, can be viewed as a scaled version $s(ct)$ of the adult $s(t)$ by a factor $c \simeq 3$ if we assume that the width of adult QRS complex is about 100 ms, $s_{nb}(t) = s(c \cdot t)$. Inserting $s(ct)$ in eqn 15, we obtain that the minimum $\sigma_{\tau_{nb}}$ for newborns has a factor $1/c$ with respect to σ_τ for adults. Accordingly, the minimum sampling frequency for newborns $f_{s_{nb}}$ must be c times larger than that for adults, i.e. $f_{s_{nb}} = c \cdot f_s$.

The present study shows from a theoretical point of view that a sampling rate of at least 3 kHz is required for accurate measurements of ensemble variability in ECG from adults. This result is further supported by experimental results obtained from a database with high-resolution ECGs, which indicate that variability measurements are reduced by an average of 40% when the sampling rate is increased from 1 to 3 kHz. It is interesting to note that such a high sampling rate is needed although the bandwidth for the ECG signals was 250 Hz. Assuming a scale factor $c = 3$ for pediatric ECGs, a sampling rate of approximately 9 kHz is required for accurate ensemble variability measurements in newborns ECGs.

Matched filtering is the classical approach to time alignment of signals in noise with unknown arrival times (VAN TREES, 1968). In this study, the Woody method was considered since it improves the performance of matched filtering by introducing an iterative procedure in which the impulse response is improved. Several other methods for time alignment of QRS complexes have been presented in the literature. For example, the normalised integral method which estimates the delay between two signals by their normalised integral difference (LAGUNA *et al.*, 1994), the sliding window method in which waveform slopes with opposite signs are detected (BARBARO *et al.*, 1991), or simple threshold crossing detection (JANÉ *et al.*, 1991). Since the performance of all three methods were, in general, inferior to that of the Woody method (LAGUNA *et al.*, 1997), the present paper considers only the Woody method for time alignment.

The use of the signal-to-noise ratio in biomedical signal processing is often problematic since the exact signal power is difficult to determine. However, the SNR is, in the present study, a useful measure to quantify noise effects when analysing a waveform $s(t)$ with known morphology. In other studies, another definition of the SNR may be preferable.

5 Conclusions

In this study, we have considered the sampling rate and the alignment effect when analysing ensemble average and ensemble variability. For an SNR of 30 dB (typical for HRECG), a sampling rate of 3 kHz is recommended so as to make the effect of time alignment negligible in EV signals. The signal can be sampled either directly at the required rate or by

interpolating the data sampled at the typical 1 kHz rate. It was shown that the EV power not only depends on misalignment but also on the frequency distribution of signal components. This aspect should be considered when studying beat-to-beat variability with the EV power measure since it depends on signal dynamics, misalignment, and the signal spectrum.

Acknowledgment—This work was supported by grant TIC97-0945-C02-01:2 and 2FD97-1197-C02-01 from CICYT, P40-98 from CONSI+D, Spain; and a grant from the Swedish National Board for Technical Developemt (NUTEK).

References

BARBARO, V., BARTOLINI, P., and FIERLI, M. (1991): 'New algorithm for the detection of ECG fiducial point in the averaging technique', *Med. Biol. Eng. Comput.*, **29**, pp. 129–135

BARR, R., and SPACH, M. (1977): 'Sampling rate required for digital recordings of intracellular and extracellular cardiac potentials', *Circulation*, **55**, pp. 40–49

BEN-HAIM, S., GIL, A., and EDOUTE, Y. (1992): 'Beat to beat morphology variability of the electrocardiogram for the evaluation of the chest pain in the emergency room', *Am. J. Cardiol.*, **70**, pp. 1139–1142

BERSON, A. (1976): 'Bandwidth sampling, and quantising for automated ECG processing', in 'Computers in cardiology' (IEEE, Piscataway, NJ), pp. 295–301

BLANCHARD, S., and BARR, S. (1985): 'Comparison of methods for adaptive sampling of cardiac electrograms and electrocardiograms', *Med. Biol. Eng. Comput.*, **23**, pp. 377–386

BREITHARDT, G., CAIN, M. E., EL-SHERIF, N., FLOWERS, N., HOMBACH, V., JANSE, M., SIMSON, M., and STEINBECK, G. (1991): 'Standards for analysis of ventricular late potentials using high resolution or signal-averaged electrocardiography', *J. Am. Coll. Cardiol.*, **17**, pp. 999–1006

GEVINS, A. S., and RÉMOND, A. (1987): 'Handbook of electroencephalography and clinical neurophysiology: methods of analysis of brain electrical and magnetic signals', volume 1 (Elsevier)

JANÉ, R., RIX, H., CAMINAL, P., and LAGUNA, P. (1991): 'Alignment methods for signal averaging of high resolution cardiac signals: a comparative study of performance', *IEEE Trans. Biomed. Eng.*, **38**, (6), pp. 571–579

LAGUNA, P., JANÉ, R., and CAMINAL, P. (1994): 'A time delay estimator based on the signal integral: Theoretical performance and testing on ECG signals', *IEEE Trans. Signal Process.* **42**, (11), pp. 3224–3229

LAGUNA, P., SIMON, B., and SÖRNMO, L. (1997): 'Improvement in high-resolution ECG analysis by interpolation before time alignment', in 'Computers in cardiology' (IEEE, Piscataway, NJ), pp. 617–620

NOWAK, J., HAGERMAN, I., YLÉN, M., NYQUIST, O., and SYLVÉN, C. (1993): 'Electrocardiogram signal variance analysis in the diagnosis of coronary artery disease–a comparison with exercise stress test in an angiographically documented high prevalence population', *Clin. Cardiol.*, **16**, pp. 671–682

PRASAD, K., and GUPTA, M. (1979): 'Phase-variant signature algorithm. A noninvasive technique for early detection and quantification of Ouabain-induced cardiac disorders', Angiology, **30**, pp. 721–732

ROMPELMAN, O., and ROS, H. H. (1986): 'Coherent averaging technique: a tutorial review. Part 1: Noise reduction and the equivalent filter. Part 2: Trigger jitter, overlapping responses and non-periodic stimulation', *J. Biomed. Eng.*, **8**, pp. 24–35

SHAW, G. R., and SAVARD, P. (1995): 'On the detection of QRS variations in the ECG', *IEEE Trans. Biomed. Eng.*, **42**, pp. 736–741

SÖRNMO, L. (1998): 'Vectorcardiographic loop alignment and morphologic beat-to-beat variability', *IEEE Trans. Biomed. Eng.*, **45**, pp. 1401–1413

SÖRNMO, L., WOHFART, B., BERG, J., and PAHLM, O. (1998): 'Beat-to-beat QRS variability in the 12-lead ECG and the detection of coronary artery disease', *J. Electrocardiol.*, **31**, pp. 336–344

UIJEN, G. J., DE WEERD, J. P., and VENDRIK, A. J. (1979): 'Accuracy of QRS detection in relation to the analysis of high-frequency components in the electrocardiogram', *Med. Biol. Eng. Comput.*, **17**, pp. 492–502

VAN TREES, H. (1968): '*Detection, estimation and modulation theory, part I*' (John Wiley & Sons, New York)

WOODY, C. (1967): 'Characterization of an adaptive filter for the analysis of variable latency neuroelectric signals', *Med. Biol. Eng.*, **5**, pp. 539–553

YAMAMOTO, H., MIYAHARA, H., and DOMAE, A. (1987): 'Is a higher sampling rate desirable in the computer processing of the pediatric electrocardiogram?', *J. Electrocardiol.*, **20**, pp. 321–328

ZYWIETZ, C., SPITZENBERGER, U., PALM, C., and WETJEN, A. (1983): 'A new approach to determine the sampling rate of ECGs', in 'Computers in cardiology' (IEEE, Piscataway, NJ), pp. 261–264

Author's biography

PABLO LAGUNA received MS and PhD degrees in Physics from the Science Faculty at the University of Zaragoza, Spain, in 1985 and 1990, respectively. The PhD thesis was developed at the Biomedical Engineering Division of the Institute of Cybernetics (U.P.C.-C.S.I.C.) under the direction of Pere Caminal. He is an associate professor of signal processing and communications in the Department of Electronics Engineering and Communications at the Centro Politécnico Superior, University of Zaragoza, Spain. From 1987 to 1992 he worked as assistant professor of automatic control in the Department of Control Engineering at the Politecnic University of Catalonia (U.P.C.), Spain and as a researcher at the Biomedical Engineering Division of the Institute of Cybernetics (U.P.C.-C.S.I.C.). His professional research interests are in signal processing, in particular applied to biomedical applications.